Combined theoretical analysis for plasmon-induced transparency in waveguide systems

Zhihui He,[1] Hongjian Li,[1,2,*] Shiping Zhan,[1] Guangtao Cao,[2] and Boxun Li[1]

[1]*College of Physics and Electronics, Central South University, Changsha 410083, China*

[2]*College of Materials Science and Engineering, Central South University, Changsha 410083, China*

**Corresponding author: lihj398@126.com*

Received June 30, 2014; revised August 12, 2014; accepted August 20, 2014;
posted August 22, 2014 (Doc. ID 213697); published September 19, 2014

We propose a novel combination of a radiation field model and the transfer matrix method (TMM) to demonstrate plasmon-induced transparency (PIT) in bright-dark mode waveguide structures. This radiation field model is more effective and convenient for describing direct coupling in bright-dark mode resonators, and is promoted to describe transmission spectra and scattering parameters quantitatively in infinite element structures by combining it with the TMM. We verify the correctness of this novel combined method through numerical simulation of the metal-dielectric-metal (MDM) waveguide side-coupled with typical bright-dark mode, H-shaped resonators; the large group index can be achieved in these periodic H-shaped resonators. These results may provide a guideline for the control of light in highly integrated optical circuits. © 2014 Optical Society of America

OCIS codes: (240.6680) Surface plasmons; (230.7370) Waveguides; (130.3120) Integrated optics devices.
http://dx.doi.org/10.1364/OL.39.005543

Plasmon-induced transparency (PIT) is an analogue of classical electromagnetically induced transparency (EIT) [1–3], which has attracted enormous attention because of its potentially important applications in the fields of slow light effects [4,5] and integrated photonic devices [6,7]. Among different plasmonic devices, metal-dielectric-metal (MDM) plasmonic waveguides have attracted much attention because they support modes with deep subwavelength scale and an acceptable propagation length for surface plasmon polaritons (SPPs). Based on the unique feature of MDM, the plasmonic analogue of EIT observed in nanoscale plasmonic resonator systems was theoretically predicted and experimentally demonstrated in recent research [8–19]. Liu *et al.* [19] used transmission line theory to introduce the subwavelength slow-light mode in periodic cut-assisted plasmonic waveguides [8,10]. However, few studies investigate bright-dark mode waveguide structures by using the transmission line theory. Cao *et al.* [17] studied the EIT-like transmission by direct and indirect couplings between two stub resonators based on temporal coupled-mode theory (CMT) [4,17], but CMT first requires the corresponding quality factor of the structure from the simulation data before seeking transmission and scattering parameters. Liu *et al.* proposed a radiation field model to demonstrate plasmonic analogue of EIT at the Drude damping limit in metamaterial structures effectively [19]. However, this model is always used to investigate optical properties of metamaterials, and very few studies discuss the PIT phenomenon in plasmonic waveguide systems by using this radiation field theory.

In this Letter, we propose a radiation field model, combined with the transfer matrix method (TMM), to demonstrate PIT in bright-dark mode waveguide structures. This radiation field model is more effective and more convenient for describing the direct coupling among bright-dark mode resonators. Moreover, a transfer matrix that is optimized is obtained in this model, then combined with the TMM is promoted to investigate transmission spectra and scattering parameters quantitatively in infinite element structures. We verify the correctness of this novel combined method through numerical simulation of a metal-dielectric-metal waveguide side-coupled with typical bright-dark mode, H-shaped resonators; obvious slow-light effects appear in our proposed structure.

In a typical bright-dark mode waveguide, the bus waveguide can be regarded as a ground state. The resonator that can be directly excited by the bus waveguide is the bright mode, and the resonator excited by the bright mode is the dark mode. We introduce a radiation field model to analyze the transmission and scattering mechanism, in which $|0\rangle$ is the ground state and $|1\rangle$ and $|2\rangle$ are the two excited states as shown in Fig. 1. $|0\rangle - |1\rangle$ defines a radiation of the bright mode. It is related to a dissipation rate γ_1. $|0\rangle - |2\rangle$ defines a radiation of dark mode and is characterized by a dissipation rate γ_2. δ denotes the detuning from the transition line center with the condition $\delta \ll \gamma_1$. The transition rate, κ, between states $|1\rangle$ and $|2\rangle$ is correlated with the coupling between the bright mode and dark mode. Consequently, the two possible pathways, namely $|0\rangle - |1\rangle$ and $|0\rangle - |1\rangle - |2\rangle - |1\rangle$, interfere destructively. A typical PIT feature appears at an originally opaque frequency range. Here, a set of two coupled harmonic oscillators can describe these systems [20],

$$\omega_1^{-2}\ddot{r}(t) + \gamma_1\omega_1^{-1}\dot{r}(t) + r(t) = f(t) - \kappa q(t), \tag{1}$$

$$\omega_2^{-2}\ddot{q}(t) + \gamma_2\omega_2^{-1}\dot{q}(t) + q(t) = \kappa r(t). \tag{2}$$

The bright resonator, with resonance frequency ω_1 and dissipation rate γ_1, is described by the excitation $r(t)$ and

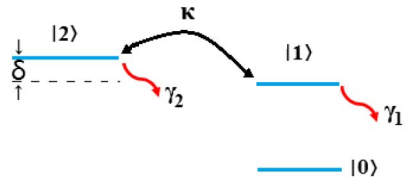

Fig. 1. Schematic of this radiation field model.

driven by the external force $f(t)$. The dark resonator, with resonance frequency ω_2 and dissipation rate γ_2, is described by the excitation $q(t)$. Both resonators are linearly coupled with coupling strength κ. Equations (1) and (2) can be solved in the frequency domain,

$$r(\omega)=\frac{[1-(\omega/\omega_2)^2-i\gamma_2(\omega/\omega_2)]\cdot f(\omega)}{[1-(\omega/\omega_2)^2-i\gamma_2(\omega/\omega_2)]\cdot[1-(\omega/\omega_1)^2-i\gamma_1(\omega/\omega_1)]-\kappa^2}. \tag{3}$$

The electric current sheet, with surface conductivity σ, is introduced to describe this effective response. The surface conductivity σ is [20],

$$\sigma\approx\frac{-i\omega[1-(\omega/\omega_2)^2-i\gamma_2(\omega/\omega_2)]}{[1-(\omega/\omega_2)^2-i\gamma_2(\omega/\omega_2)]\cdot[1-(\omega/\omega_1)^2-i\gamma_1(\omega/\omega_1)]-\kappa^2}. \tag{4}$$

So the transmission and reflection can be calculated in following form [20],

$$T=\left|\frac{2}{2+\zeta\sigma}\right|^2 \qquad R=\left|\frac{\zeta\sigma}{2+\zeta\sigma}\right|^2, \tag{5}$$

where $\zeta=\beta(b)b/\omega\varepsilon_0\varepsilon_1$ [21] is the wave impedance of the external waves, ε_0 is the permittivity of the vacuum, and ε_1 is the relative permittivity of the filled medium in the resonators. $\beta(b)$ is a propagation constant in MDM resonators, and b is the width of the MDM resonator.

To verify the theoretical analysis above, we proposed a MDM waveguide side-coupled with periodic H-shaped resonators as shown in Fig. 2(a) where p is the period of our proposed structure. Each unit cell consists of three identical rectangular resonators in which $b=50$ nm is the width for both bus waveguide and rectangular resonators, $a=250$ nm is the length of the rectangular resonator, $S=20$ nm, and d_i is the separation distance between the bus waveguide and the center line of the horizontal rectangular resonator. The background metal is chosen to be silver (Ag), for which the frequency-dependent complex permittivity ε_m is approximately defined by the Drude model as $\varepsilon(\omega)=\varepsilon_\infty-\omega_p^2/(\omega^2+i\omega\gamma_p)$, where ω stands for the angular frequency of the incident wave, $\omega_p=1.38\times10^{16}$ rad/s is the bulk plasmon frequency, and $\gamma_p=2.73\times10^{13}$ rad/s represents the damping rate, which characterizes the absorption loss. The white part is air with permittivity $\varepsilon_a=1$ for simplicity. The characteristic spectral responses of the structures are found using the two-dimensional finite difference time-domain (FDTD) method. The calculation domain is divided into uniform Yee cells and surrounded by the perfectly matched layer (PML) absorbing boundary. In this unit cell of our proposed structure, the two vertical rectangular resonators are directly excited by the bus waveguide, so the vertical rectangular resonators can be regarded as bright modes. However, the horizontal rectangular resonator is excited by the bright modes; thus, it is a dark mode. Both the simulative and theoretical transmission spectra for the waveguide coupled to only one H-shaped resonator with different d_1 are plotted in Fig. 2(b). When $d_1=145$ nm, the dark mode resonator

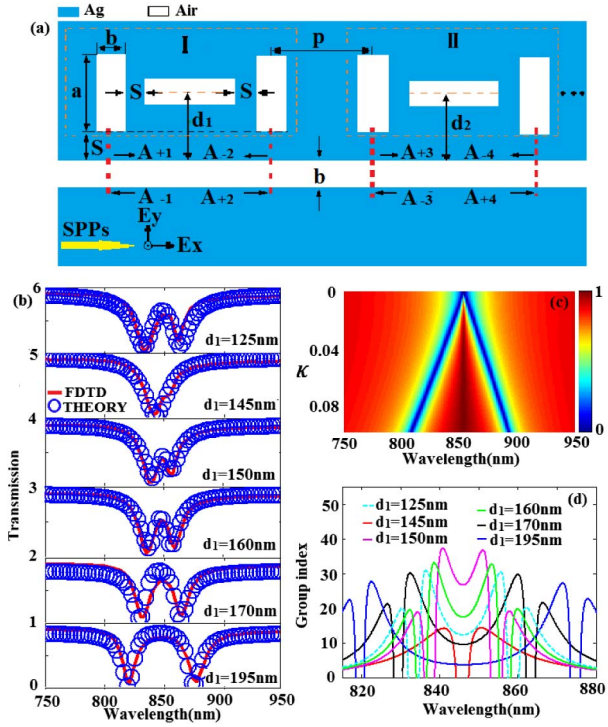

Fig. 2. (a) Schematic of MDM waveguide coupled to H-shaped resonators; (b) Transmission spectra with different coupling distance d_1; (c) Evolution of the transmission spectra versus κ and λ; (d) Group index in the plasmonic waveguide for distance d_1.

aims at the middle of the bright modes, so the dark mode is almost not excited [19] as it shows one dip in the transmission spectrum. With the increase of d_1, a typical PIT feature is observed in the transmission spectra when structural asymmetry appears [22] because two different resonant modes interfere destructively in this asymmetric structure. As d_1 increases from 145 to 195 nm, the full width at half-maximum (FWHM) of the transparency window shows an increasing trend. It is observed that the transmission spectra also shows the PIT feature when $d_1=125$ nm. However, d_1 cannot be smaller than 125 nm in our proposed structure because there are interactions that cannot be ignored between bus waveguide and the dark mode resonator when $d_1<125$ nm, which are in good agreement with the FDTD results marked as a red solid line. This conclusion provides a convenient tuning of PIT, which may guarantee a wider application in integrated plasmonic devices. Figure 2(c) is an evolution of the transmission spectra versus κ and λ, which agrees with Fig. 2(b). This gives additional support to the fact that the PIT effect is realized in different separations. The slow-light effects are also investigated in this waveguide structure as shown in Fig. 2(d) where the group index $n_g=c/L(d\psi/d\omega)$, ψ is transmission phase, $L=500$ nm is the length of the bus waveguide, and c is the velocity of light in vacuum. It is observed that the group index at the transmission peak first increases and then decreases as d_1 increases from 145 to 195 nm. This result may be helpful for us to design the plasmonic slow-light device.

In order to expand the application range of this radiation field model, we apply this theoretical deriva-

tion to the bus waveguide side-coupled with multiple resonators. The TMM is introduced to analyze the transmission properties in the transparency window. According to this method, the transmission lines are related by the matrix equation,

$$T_N\begin{pmatrix} A_{+1} \\ A_{-1} \end{pmatrix} = \begin{pmatrix} A_{+2N} \\ A_{-2N} \end{pmatrix}, \tag{6}$$

where the transfer matrix is given by

$$T_N = (M_N P)\cdot(M_{N-1}P)\cdots(M_2 P)\cdot M_1 \tag{7}$$

with

$$M_i = \begin{bmatrix} 1 & 1 \\ \xi_i\sigma_i & 2+\xi_i\sigma_i \end{bmatrix} \qquad P = \begin{bmatrix} \exp^{-iKp} & 0 \\ 0 & \exp^{-iKp} \end{bmatrix}, \tag{8}$$

where $K = \alpha + i\beta$ is the Bloch wave vector, So the transmittance of the MDM waveguide coupled to N unit structure is found to be

$$T_N = \left|\frac{A_{+2N}}{A_{+1}}\right|^2. \tag{9}$$

To further illustrate the accuracy of our theory, we apply this theoretical derivation to the bus waveguide side-coupled with two H-shaped resonators. When $N = 2$, the transmittance of the MDM waveguide coupled to the two-unit structure is

$$T_2 = \left|\frac{A_{+4}}{A_{+1}}\right|^2 = \left|\frac{4}{\xi_1\sigma_1 + (\xi_1\sigma_1+2)(\xi_2\sigma_2+2)}\right|^2 \cdot \exp(-2iKp). \tag{10}$$

In Fig. 3, we have plotted the FDTD simulation and the theoretical transmission spectra as a function of the distance d_2 in the second H-shaped resonator. We find that the transmission spectra of the simulation data [Fig. 3(a)] is in agreement with the theory data [Fig. 3(b)]. The reason of the discrepancy between Figs. 3(a) and 3(b) at 900 nm is that the interaction among these two H-shaped resonators is ignored. These studies not only verify the theoretical analysis above, but also combine the

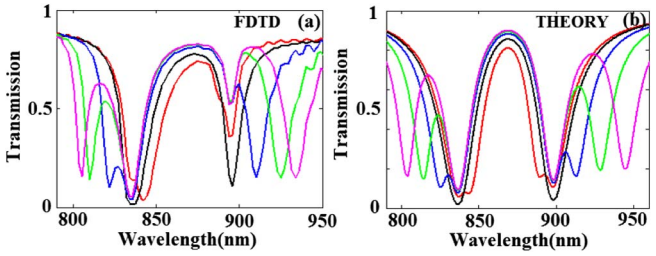

Fig. 3. (a) and (b) Transmission spectra of the simulation data and theory data in the bus waveguide side-coupled with two H-shaped resonators with $p = 100$ nm; $d_1 = 170$ nm and $d_2 = 145$ nm (red curve); 170 nm (black curve); 195 nm (blue curve); 220 nm (green curve); and 250 nm (pink curve), respectively.

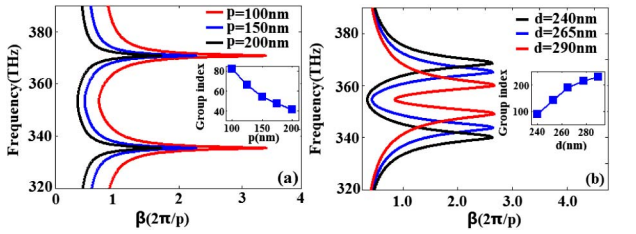

Fig. 4. (a) Dispersion relation of system with $p = 100$, 150, 200 nm, respectively. The inset is n_g as a function of period p. (b) Dispersion relation of system with $d = 240$, 265, 290 nm, respectively. The inset is n_g as a function of d.

radiation field model and the TMM perfectly. Moreover, they provide a new idea for future research.

In this section, we discuss the dispersion relation of a periodic system with the unit cell mentioned above. Based on the Bloch theory, which is widely cited in the literature [23], we calculate the propagation constant, β, for the periodic structure and the corresponding determinant should satisfy the formula

$$|M - IP| = 0, \tag{11}$$

where I represents the unit matrix. Since matrices M and P are given in the equation (8), the dispersion relation of the whole system can be derived as

$$e^{-2iKp} - (3+\xi\sigma)e^{-iKp} + 2 = 0. \tag{12}$$

The dispersion relation of the system with $p = 100$, 150, and 200 nm is plotted in Fig. 4(a). Here the frequency unit THz for the vertical axis is used in the following discussion for clarity. The band between frequency 320 and 390 THz corresponds to a mode with slow group velocity $v_g = \partial\omega/\partial\beta$. We can consider that the slope at a point on the curve approximately represents the corresponding v_g at this frequency. Then, we infer that the group index n_g around the transparency peak at 355 THz (~845.1 nm) for $p = 100$ nm is larger than that for $p = 200$ nm due to the smaller slope. In addition, the dispersion relation of the system as a function of distance d ($d = d_i$) is considered in our Letter. The group index n_g at 355 THz for d ranging from 240 to 290 nm is plotted in the inset of Fig. 4(b). It is observed that the group index increases as d increases. In addition, when the parameter $d > 280$ nm, the group index increases slowly. So far, we have presented a convenient way to adjust the n_g for a given frequency by changing the distance d and period p in a periodic waveguide system.

In summary, we have demonstrated PIT in plasmonic waveguide structures effectively and conveniently through combining this radiation field model and the TMM. The consistency between the theoretical and numerical results validates the correctness of the combined theoretical description. In addition, the dispersion relation of our proposed structure with period p or distance d is discussed by this combined method in detail, and the large group index can be achieved. The results may open up an avenue for designing nanoscale optical switching, ultrasensitive sensors and slow-light devices in highly integrated optical circuits.

This work was funded by the Research Fund for the Doctoral Program of Higher Education of China under Grant No. 20100162110068 and the National Natural Science Foundations of China under Grant No. 61275174.

References

1. C. Kurter, P. Tassin, L. Zhang, T. Koschny, A. Zhuravel, A. Ustinov, S. Anlage, and C. Soukoulis, Phys. Rev. Lett. **107**, 043901 (2011).
2. Z. Chai, X. Hu, Y. Zhu, F. Zhang, H. Yang, and Q. Gong, Appl. Phys. Lett **102**, 201119 (2013).
3. S. Zhang, D. A. Genov, Y. Wang, M. Liu, and X. Zhang, Phys. Rev. Lett. **101**, 047401 (2008).
4. G. Cao, H. Li, S. Zhan, Z. He, Z. Guo, X. Xu, and H. Yang, Opt. Lett. **39**, 000216 (2014).
5. R. Hokari, Y. Kanamori, and K. Hane, Opt. Express **22**, 3526 (2014).
6. J. Zhang, W. Bai, L. Cai, Y. Xu, G. Song, and Q. Gan, Appl. Phys. Lett. **99**, 181120 (2011).
7. Y. Zhu, X. Hu, H. Yang, and Q. Gong, Sci. Rep. **4**, 03752 (2014).
8. G. Wang, H. Lu, and X. Liu, Appl. Phys. Lett. **101**, 013111 (2012).
9. Z. Han and S. Bozhevolnyi, Opt. Express **19**, 3251 (2011).
10. G. Wang, H. Lu, and X. Liu, Opt. Express **20**, 20902 (2012).
11. H. Lu, X. Liu, and D. Mao, Phys. Rev. A **85**, 053803 (2012).
12. H. Lu, X. M. Liu, D. Mao, Y. K. Gong, and G. X. Wang, Opt. Lett. **36**, 3233 (2011).
13. X. Piao, S. Yu, S. Koo, K. Lee, and N. Park, Opt. Express **19**, 10907 (2011).
14. Y. Guo, L. Yan, W. Pan, B. Luo, K. Wen, Z. Guo, and X. Luo, Opt. Express **20**, 24348 (2012).
15. R. Kekatpure, Phys. Rev. Lett. **104**, 243902 (2010).
16. H. Haus and W. Huang, Proc. IEEE **79**, 1505 (1991).
17. G. Cao, H. Li, S. Zhan, H. Xu, Z. Liu, Z. He, and Y. Wang, Opt. Express **21**, 9198 (2013).
18. L. Chen, C. Gao, J. Xu, X. Zang, B. Cai, and Y. Zhu, Opt. Lett. **38**, 1379 (2013).
19. N. Liu, L. Langguth, T. Weiss, J. Käste, M. Fleischhauer, T. Pfau, and H. Giessen, Nat. Mater. **8**, 758 (2009).
20. P. Tassin, L. Zhang, R. Zhao, A. Jain, T. Koschny, and C. M. Soukoulis, Phys. Rev. Lett. **109**, 187401 (2012).
21. P. Asanka, D. Ivan, P. Malin, T. Haroldo, and P. Govind, Opt. Express **18**, 6191 (2010).
22. Z. Dong, H. Liu, M. Xu, T. Li, S. Wang, J. Cao, S. Zhu, and X. Zhang, Opt. Express **18**, 22412 (2010).
23. S. Zhan, H. Li, G. Cao, Z. He, B. Li, and H. Yang, J. Phys. D **47**, 205101 (2014).